Zhang *et al. One Health Advances* (2024) 2:20
https://doi.org/10.1186/s44280-024-00056-w

One Health Advances

ARTICLE

Open Access

Ellagic acid supplementation ameliorates cisplatin-induced liver injury in mice by inhibiting the NF-κB pathway and activating the Nrf2/HO-1 pathway

Xueyong Zhang[1,2], Yue Liu[1,2], Mingchao Liu[3], Qiang Ma[1,2], Zhihui Hao[1], Shusheng Tang[1,2] and Chongshan Dai[1,2*]

Abstract

Cisplatin (cis-diaminodichloroplatinum II, CDDP), an essential chemotherapeutic agent, can cause potential hepatotoxicity, but the underlying molecular mechanisms remain unclear. In this study, the protective effects of ellagic acid (EA) on CDDP exposure-induced hepatotoxicity and the underlying molecular mechanisms were investigated in a mouse model. Mice were randomly divided into control, CDDP model, EA100 (i.e., 100 mg/kg/day), and CDDP plus 25, 50, or 100 mg/kg/day EA groups. Mice in all the CDDP-treated groups were intraperitoneally injected with 20 mg/kg/day CDDP for two days. For all EA cotreatments, the mice were orally administered EA for seven days. Our results revealed that CDDP treatment resulted in liver dysfunction, oxidative stress, and caspase activation, which were effectively attenuated by EA cotreatment in a dose-dependent manner. Furthermore, EA supplementation significantly downregulated the CDDP exposure-induced protein and mRNA expression of NF-κB, IL-1β, TNF-α, and IL-6 but further upregulated the protein and mRNA expression of Nrf2 and HO-1. Molecular docking analysis revealed strong interactions between EA and the NF-κB or Keap1 proteins. In conclusion, our results revealed that EA supplementation could ameliorate CDDP-induced liver toxicity in mice by activating the Nrf2/HO-1 signaling pathway and inhibiting the NF-kB signaling pathway.

Keywords Ellagic acid, Cisplatin, Hepatotoxicity, Nrf2/HO-1 signaling pathway, NF-κB signaling pathway

Introduction

Cisplatin (cis-diamminedichloroplatinum II, CDDP) is an anticancer-based drug that is widely used for treating human malignancies, such as sarcomas, malignant epithelial tumors, lymphoma, and germ cell tumors [1]. In clinical practice, CDDP treatment usually causes certain toxic effects and adverse effects, such as neurotoxicity, nephrotoxicity, hepatotoxicity, and reproductive toxicity [2–5]. These unwanted adverse effects usually limit its clinical application and outcomes. Therefore, investigations on the molecular mechanisms underlying the adverse effects of CDDP and the development of effective protective agents are essential and urgent.

*Correspondence:
Chongshan Dai
daichongshan@cau.edu.cn
[1] National Key Laboratory of Veterinary Public Health and Safety, College of Veterinary Medicine, China Agricultural University, Beijing 100193, China
[2] Beijing Key Laboratory of Detection Technology for Animal-Derived Food Safety, China Agricultural University, Beijing 100193, China
[3] College of Veterinary Medicine, Hebei Agricultural University, Baoding 071001, China

It has been reported that CDDP can directly crosslink with the purine bases of DNA or damage DNA via the induction of excessive reactive oxygen species (ROS) production, ultimately resulting in mitosis and cell apoptosis in multiple cancer cells [6]. In mammalian cells, the liver is the main organ where most metabolic reactions occur. CDDP can rapidly reach a high concentration in the liver of patients and cause acute liver injury [6]. To date, there have been reports of various stress responses, including cell cycle arrest, aging, autophagy, programmed necrosis, cell apoptosis, and inflammation, that play critical roles in the pathogenesis of cisplatin-induced tissue injury [3]. It was reported that CDDP exposure could significantly decrease the levels of reduced glutathione (GSH) and increase the levels of malondialdehyde (MDA), resulting in oxidative stress and liver injury. CDDP exposure can significantly promote the expression of nuclear factor-κB (NF-κB) and subsequently increase the levels of interleukin (IL-1β), tumor necrosis factor (TNF-α), and nitric oxide synthetase (iNOS), ultimately triggering an inflammatory response in the liver tissues of rats [7]. Adaptationally, it was reported that CDDP exposure can upregulate the expression of nuclear factor erythroid 2-related factor 2 (Nrf2), phospho (p)-extracellular signal-regulated kinase (p-ERK1/2), heme oxygenase (HO)-1, Bax, caspase-3, p-p38, and p–c-Jun N-terminal kinase (p-JNK) proteins in the liver tissues of rodents, indicating that Nrf2, mitochondrial apoptotic, and mitogen-activated protein kinase (MAPK) pathways participate in CDDP-induced hepatotoxicity [8–13]. Ferroptosis, a new form of cell death, has been demonstrated to be involved in CDDP-induced cytotoxicity and nephrotoxicity [14]. Overall, these findings provide potential targets for preventing or treating the potential adverse effects caused by CDDP in clinical practice.

In animal models, several studies have shown that oral supplementation of silymarin can effectively reduce CDDP-induced hepatotoxicity, muscle atrophy, ototoxicity, and nephrotoxicity both in vivo and in vitro [15–18]. To date, there is still a lack of effective evidence for the protective effect of ellagic acid (EA; Fig. S1) on cisplatin-induced hepatotoxicity. EA is a polyphenolic compound that can be isolated from various gallnuts and fruits, such as black currants, pomegranates, raspberries, and mangos [19]. EA possesses multiple pharmacological activities, such as anticancer, anti-oxidative stress, anti-inflammatory, antibacterial, and antiaging activities [20–26]. Qi et al. reported that oral administration of EA at various doses (i.e., 50, 100, or 200 mg/kg/day) for three weeks (i.e., 21 days) improved paraquat exposure-induced inflammatory cell infiltration, oxidative stress, and apoptotic cell death in the livers of pigs by enhancing the gut microbial profile [27]. In another study, Aslan and colleagues found that EA supplementation could effectively attenuate chronic exposure to carbon tetrachloride (CCl_4)-induced liver and kidney injuries in rats via the inhibition of oxidative stress through upregulating the Nrf2 pathway and downregulating the NF-κB pathway [28, 29]. To date, the protective effects of EA against CDDP-induced hepatotoxicity and the potential actional mechanisms are not clarified. Therefore, in the present study, we investigated the interventional effects of EA supplementation on CDDP exposure-induced liver toxicity and the key actional mechanisms using a mouse model.

Results

Effects of EA supplementation on the liver index and function

During the experiments, no mouse died. CDDP treatment significantly decreased the relative liver weight, and this effect was effectively reversed by EA supplementation (Fig. S2).

Compared to those in the untreated control group, marked liver dysfunction was detected in the CDDP model group, with significantly increased serum alanine transaminase (ALT) (increased to 48.7 U/L; $p < 0.001$) and aspartate transaminase (AST) (increased to 78.7 U/L; $p < 0.001$) levels (Fig. 1). EA supplementation significantly decreased CDDP exposure-induced liver toxicity. Compared with those in the CDDP alone treatment group, the serum ALT levels in the CDDP plus 25, 50, and 100 mg/kg/day EA groups were decreased to 42.7 U/L, 31.3 U/L ($p < 0.001$), and 29.8 U/L ($p < 0.001$), respectively; and the serum AST levels were decreased to 67.8 U/L, 53.3 U/L ($p < 0.001$), and 48.8 U/L ($p < 0.001$), respectively (Fig. 1). Compared to those in the untreated control group, EA alone treatment did not alter the levels of serum ALT and AST (Fig. 1).

EA supplementation attenuates CDDP exposure-induced histopathological damage in the liver

Compared to the untreated control group, CDDP-treated mice exhibited marked histopathological injury to the liver. As shown in Fig. 2, marked central venous congestion with a few necroses and inflammatory cell infiltration were detected in the livers of CDDP-treated mice. Similarly, the number of SQSs significantly increased to 2.5 ($p < 0.001$). EA co-treatments at 50 and 100 mg/kg per day for seven days markedly reduced CDDP exposure-induced liver injury, and the SQSs were significantly decreased to 1.3 ($p < 0.05$) and 0.8 ($p < 0.01$), respectively. No marked histopathological injury was observed in the group treated with EA alone treatment group, compared to the vehicle treatment group (Fig. 2).

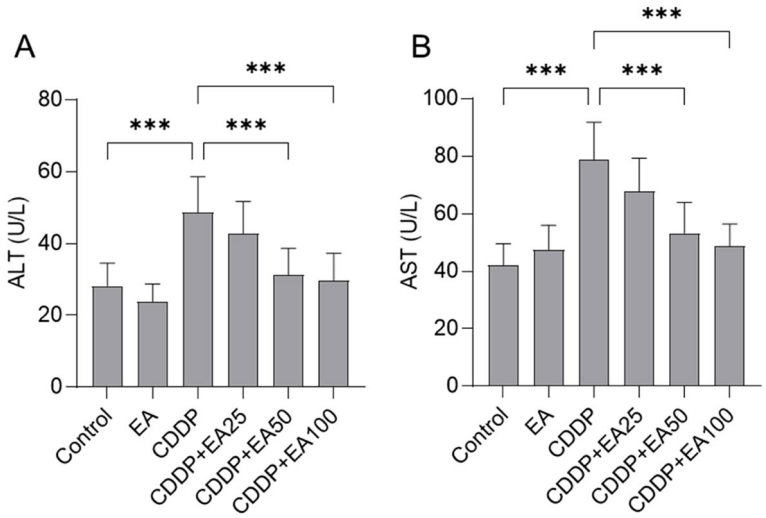

Fig. 1 Effects of EA supplementation on serum ALT **A** and AST **B** levels in CDDP-treated mice. The results are presented as the mean ± S.D. ($n = 8$). Compared between 2 groups, *** $p < 0.001$. EA: ellagic acid; ALT: alanine transaminase; AST: aspartate transferase; CDDP: cis-diamminedichloroplatinum II

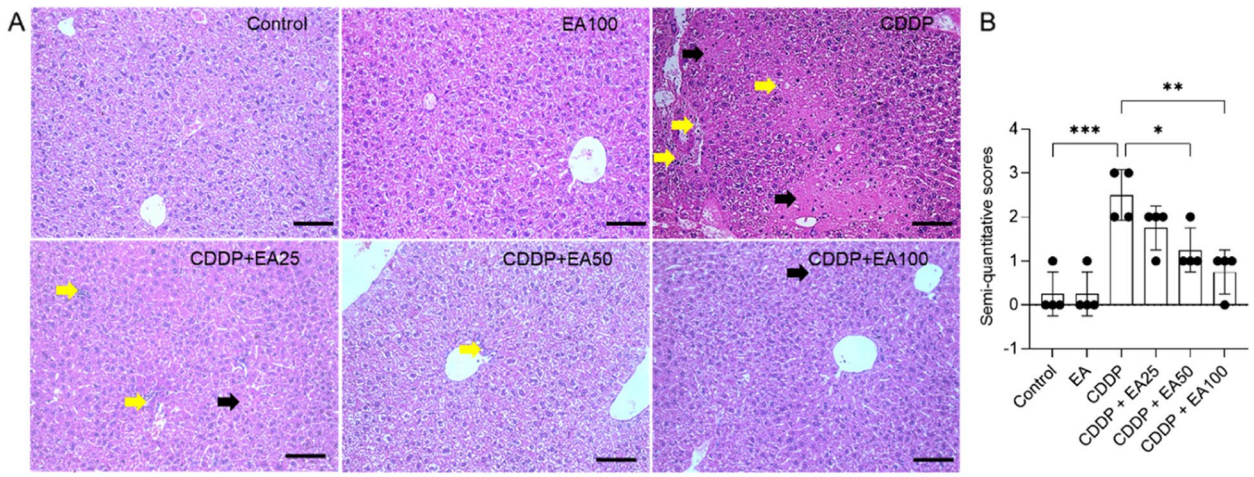

Fig. 2 EA supplementation attenuates CDDP-induced pathological injury in the liver. Representative H&E images (**A**) and semiquantitative scores (SQSs) (**B**) are presented. The results are presented as the mean ± S.D. ($n = 4$). A comparison between any two groups were performed, *$p < 0.05$, **$p < 0.01$, and *** $p < 0.001$. Scale bar = 50 μm. Yellow arrow, inflammatory cell infiltration; black arrow, hepatocyte necrosis

EA supplementation attenuates CDDP exposure-induced liver oxidative stress damage

Compared to vehicle treatment, CDDP treatment alone significantly increased the malondialdehyde (MDA) to 2.5 nmol/mg protein ($p < 0.001$) and decreased the catalase (CAT) and superoxide dismutase (SOD) activities to 83.3 U/mg protein and 79.3 U/mg protein (both $p < 0.001$), respectively (Fig. 3). EA co-treatment markedly attenuated CDDP exposure-induced increases in MDA levels and decreases in SOD and CAT activities in the livers. In the CDDP plus EA50 and EA100 groups, the MDA levels were significantly decreased to 2.2 nmol/mg protein and 1.9 nmol/mg protein ($p < 0.01$ or 0.001), respectively (Fig. 3A); the CAT activities were markedly increased to 97.8 U/mg protein and 108.4 U/mg protein ($p < 0.01$ or 0.001), respectively (Fig. 3B); and the SOD activities were significantly increased to 100.3 U/mg protein and 106.1 U/mg protein (both $p < 0.001$), respectively (Fig. 3C).

EA supplementation attenuates the CDDP exposure-induced inflammatory response in the livers of mice

The levels of the IL-1β, TNF-α, and IL-6 proteins in the livers of CDDP-treated mice were significantly increased

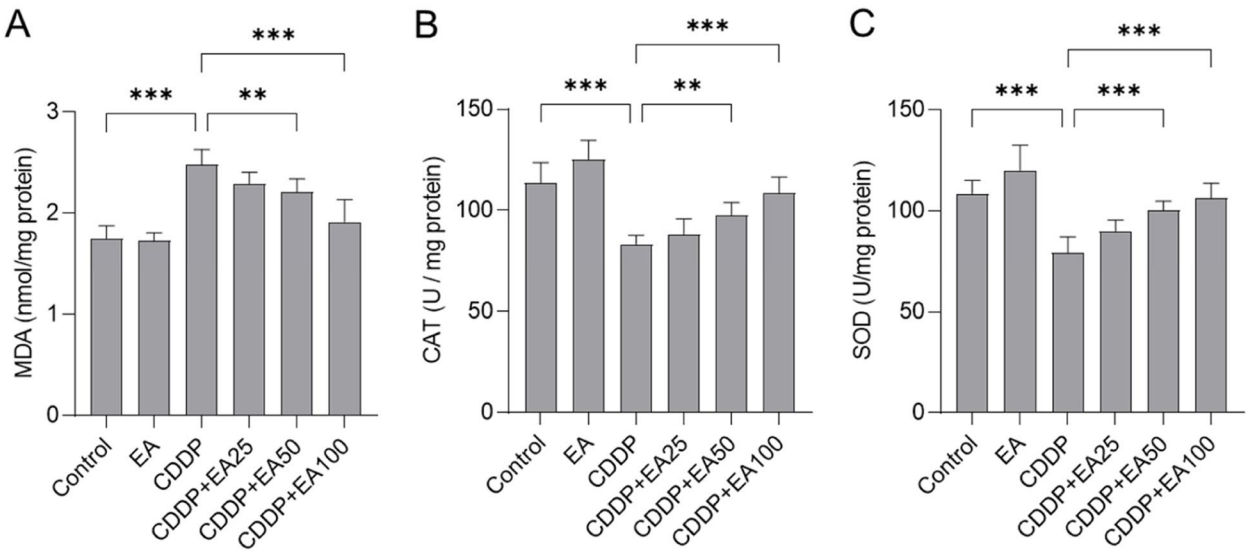

Fig. 3 Changes in the MDA levels (**A**) and CAT (**B**) and SOD (**C**) activities in the livers of the mice. The results are shown as the mean ± S.D. ($n = 8$). A comparison between any two groups were performed, *$p < 0.05$, **$p < 0.01$, and *** $p < 0.001$. MDA: Malondialdehyde; CAT: Catalase; SOD: Superoxide dismutase

to 90.8 pg/mg protein, 24.1 pg/mg protein, and 74.3 pg/mg protein (all $p < 0.001$), respectively (Fig. S3). EA cotreatment significantly decreased the levels of these inflammatory markers. In the CDDP plus EA50 and CDDP plus EA100 groups, the levels of IL-1β protein were significantly decreased to 69.3 pg/mg protein and 51.2 pg/mg protein ($p < 0.01$ or 0.001) (Fig. S3A), respectively; the levels of TNF-a protein were significantly decreased to 16.2 pg/mg protein and 13.6 pg/mg protein ($p < 0.01$ or 0.001) (Fig. S3B), respectively; and the levels of IL-6 protein were significantly decreased to 56.2 pg/mg protein and 47.8 pg/mg protein (both $p < 0.001$), respectively (Fig. S3C). Compared to vehicle treatment group, EA alone treatment did not affect the expression of IL-1β, TNF-α, or IL-6 proteins in the livers (Fig. S3).

EA supplementation attenuates CDDP exposure-induced activation of casapses in the liver

As shown in Fig. S4, the activities of caspase-9 and caspase-3 in the livers of CDDP-treated mice significantly increased by 3.1- and 3.2-fold (both $p < 0.001$), respectively, compared to that in the control group. Oral administration of 50 or 100 mg/kg EA per day for seven days effectively attenuated the CDDP exposure-induced upregulation of caspase-9 and caspase-3 in the livers of mice. In the CDDP plus EA50 group, the activities of caspase-9 and caspase-3 were significantly decreased to 1.6- and 1.9-fold (both $p < 0.001$), respectively; in the CDDP plus EA100 group, the activities of caspase-9 and caspase-3 were significantly decreased to 1.1- and 1.4-fold (both $p < 0.001$), respectively. Compared to vehicle treatment group, EA alone treatment did not alter the activities of caspase-9 and caspase-3 in the livers (Fig. S4).

EA supplementation upregulates the expression of Nrf2 and HO-1 mRNAs and downregulates the expression of p65NF-kB, IL-1β, TNF-α, and IL-6 mRNAs in the livers of mice

The expression of p65NF-kB, IL-1β, TNF-α, IL-6, Nrf2, and HO-1 mRNAs in the livers was determined. Compared to those in the untreated control group, CDDP exposure markedly increased the expression of all genes, i.e., the expression of p65NF-kB, IL-1β, TNF-α, IL-6, Nrf2, and HO-1 mRNAs increased 3.7-, 3.7-, 4.2-, 3.4-, 1.6-, and 2.3-fold (all $p < 0.001$), respectively (Fig. 4). EA supplementation regulated the expression of these genes. Specifically, in the CDDP plus EA100 group, the expression of p65NF-kB, IL-1β, TNF-α, and IL-6 mRNAs decreased 1.6-, 1.7-, 1.6-, and 1.7-fold (all $p < 0.001$), respectively, while the expression of Nrf2 and HO-1 mRNAs increased 2.3- and 3.5-fold (both $p < 0.001$), respectively, compared to that in the CDDP-treated group. Moreover, EA treatment alone significantly increased the expression of Nrf2 and HO-1 mRNAs by 1.8- and 2.0-fold (both $p < 0.01$), respectively. EA alone treatment had a minor effect on the expression of the p65NF-kB, IL-1β, TNF-α, and IL-6 mRNAs compared to those in the livers of the vehicle-treated mice (Fig. 4).

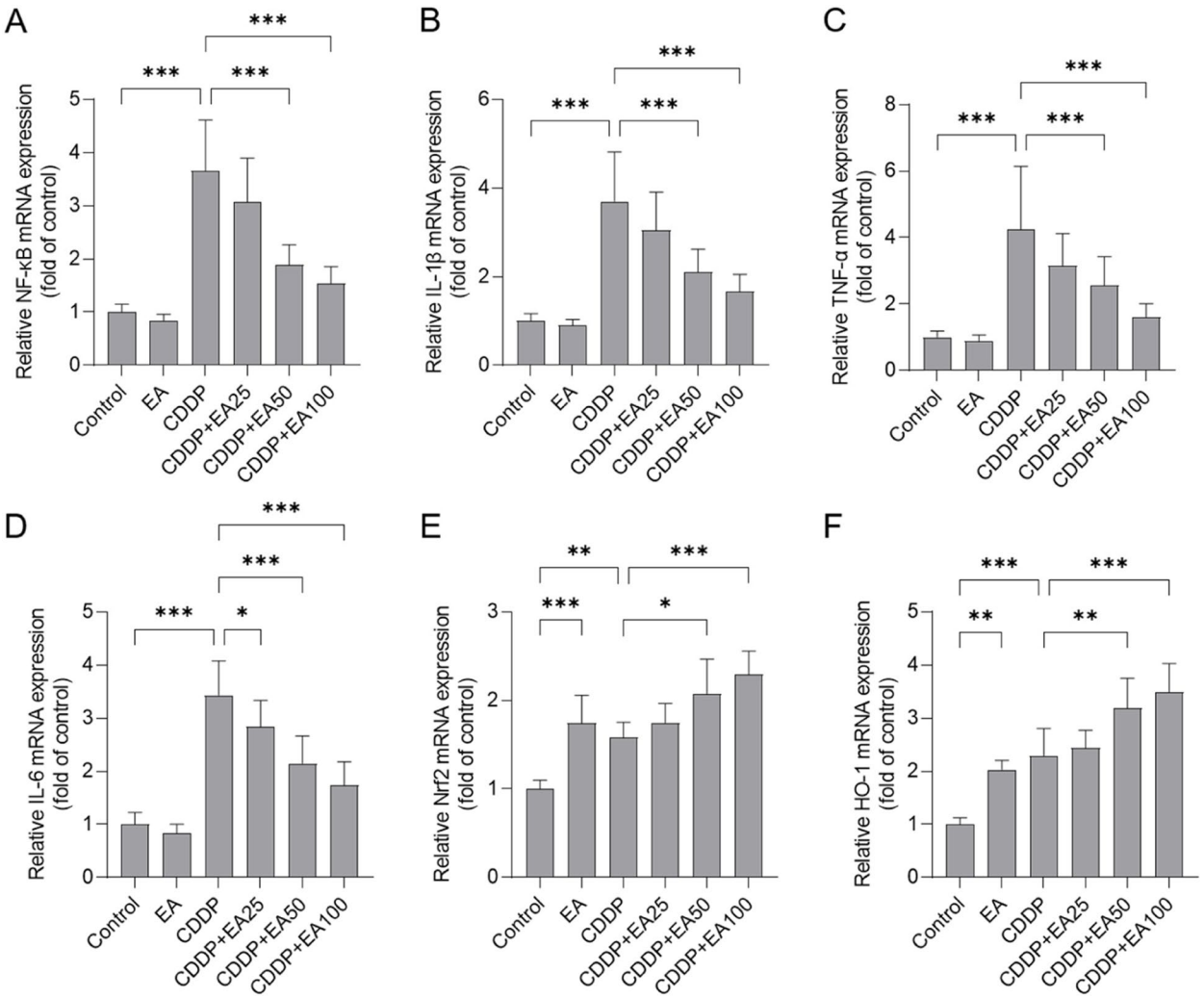

Fig. 4 The relative levels of p65NF-κB (**A**), IL-1β (**B**), TNF-α (**C**), IL-6 (**D**), Nrf2 (**E**), and HO-1 (**F**) mRNAs in the livers of the mice. The results are presented as the mean ± S.D. ($n = 6$). Compared between 2 groups, * $p < 0.05$, ** $p < 0.01$, and *** $p < 0.001$

EA supplementation promotes the protein expression of Nrf2 and HO-1 and inhibits the protein expression of NF-kB p65 in the livers of mice

Compared to those in the control group, the Nrf2, HO-1, and p65NF-kB protein levels were significantly increased by 1.9-fold ($p < 0.05$), 2.0-fold ($p < 0.05$), and 4.2-fold ($p < 0.001$) (Fig. 5), respectively. EA co-treatment further increased the protein expression of Nrf2 and HO-1 but significantly inhibited the protein expression of p65NF-kB (Fig. 5). In the CDDP plus EA 50 and EA 100 groups, the expression of Nrf2 protein in the liver significantly increased to 2.9- and 4.0-fold ($p < 0.01$ or 0.001), respectively; the expression of HO-1 protein significantly increased to 3.0- and 4.2-fold ($p < 0.05$ or 0.001), respectively; and the expression of p65NF-kB protein significantly decreased to 1.7- and 1.6-fold (both $p < 0.001$), respectively, compared to that in the CDDP alone treatment group (Fig. 5).

Molecular docking analysis of EA with the Nrf2, Keap1, and p65 NF-κB proteins

The affinity of EA for the Nrf2, Keap1, and p65NF-kB proteins was evaluated by the molecular docking analysis method. As shown in Fig. 6, the binding energies of EA to the Keap1 and p65NF-kB proteins were lower (i.e., their binding energies were −9.2 and −9.0 kcal/mol, respectively) than those of EA to the Nrf2 protein (i.e., the binding energy was −6.4 kcal/mol), indicating that EA had more stable binding with the Keap1 and p65NF-kB proteins than with the Nrf2 protein (Fig. 6A). We further found that the binding of EA to Keap1 (Fig. 6B) and p65NF-kB (Fig. 6C) may involve visible hydrogen bonds and strong electrostatic interactions.

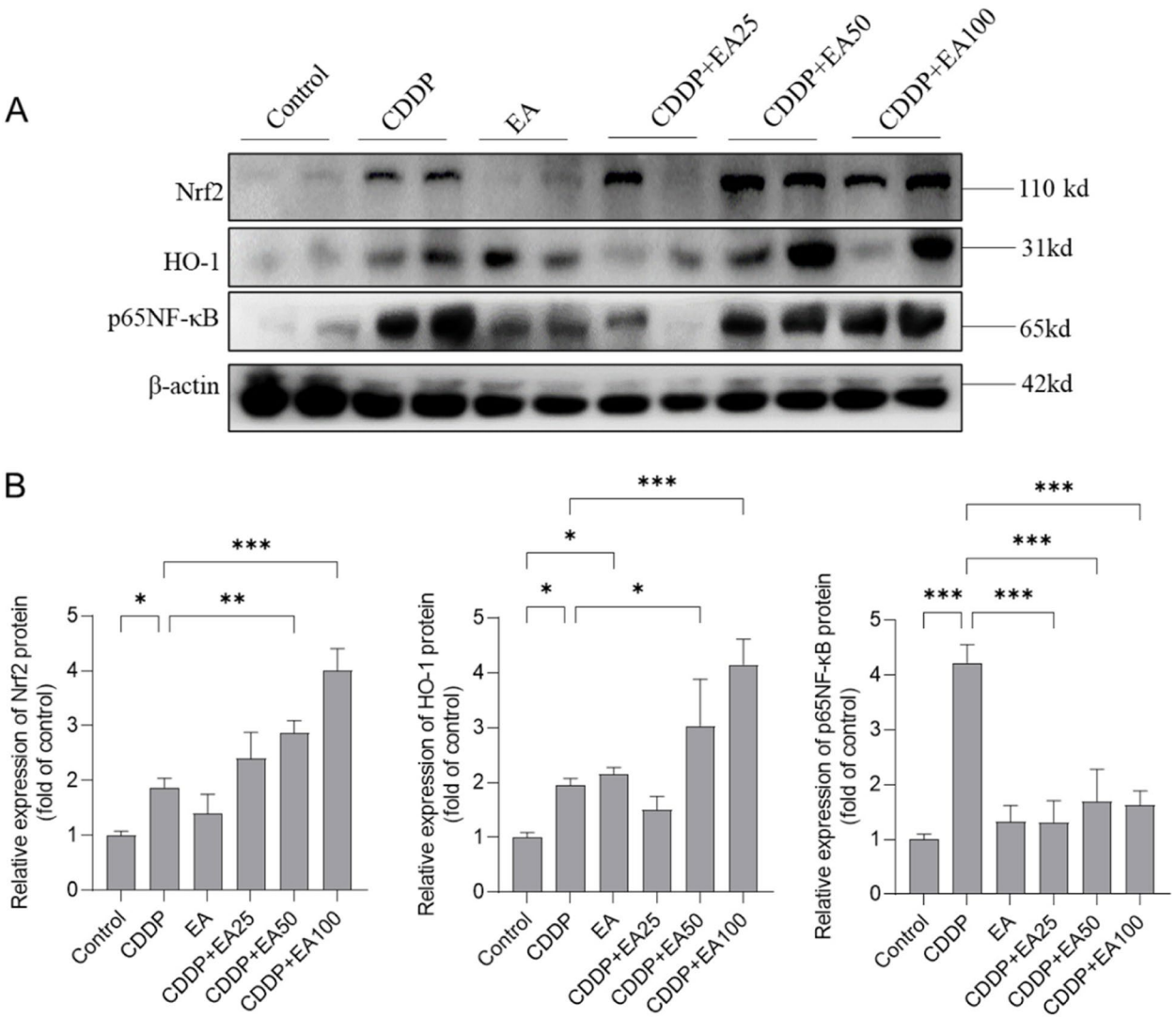

Fig. 5 The results of western blotting analysis in the liver tissues. Representative images of Western blots (**A**) and the quantitative analysis (**B**) were shown ($n=4$). Compared between 2 groups, * $p<0.05$, ** $p<0.01$, and *** $p<0.001$

Discussion

Liver toxicity is one of multiple adverse effects in patients during CDDP treatment [13]. Our current results revealed that intraperitoneal CDDP administration at 20 mg/kg/day for two days (i.e., a cumulative dose of 40 mg/kg) significantly increased the serum AST and ALT levels in mice, indicating that liver injury occurred (Fig. 1). In addition, marked histopathological changes, including hepatocyte necrosis, inflammatory cell infiltration, and central venous congestion, were detected in CDDP-treated liver tissues (Fig. 2). Furthermore, our current results showed that CDDP exposure-induced liver injury involves changes in inflammatory and oxidative stress biomarkers (Figs. 2–5), indicating that the inflammatory response and oxidative damage play critical roles in CDDP-induced liver toxicity in mice, which is in line with previous studies [13, 30].

EA is a plant phenolic compound. It can be isolated from various fruits, such as strawberries, pomegranate, and almond [27]. EA possesses various pharmacological activity, including anti-aging, anti-inflammatory, antioxidant, and anti-infection effects [20–26]. Several previous studies have shown that EA supplementation can improve the cytotoxicity and liver toxicity induced by drugs (such as doxorubicin hydrochloride and fluoxetine) and toxins (such as CCl_4, lipopolysaccharide [LPS]/d-galactosamine, hexavalent chromium, and alcohol) by inhibiting oxidative stress, apoptosis, and

A

Protein names	Uniport information	Binding Energy (kcal/mol)
Keap1	Q9Z2X8	-9.2
p65NF-κB	P25799	-8.2
Nrf2	Q60795	-6.4

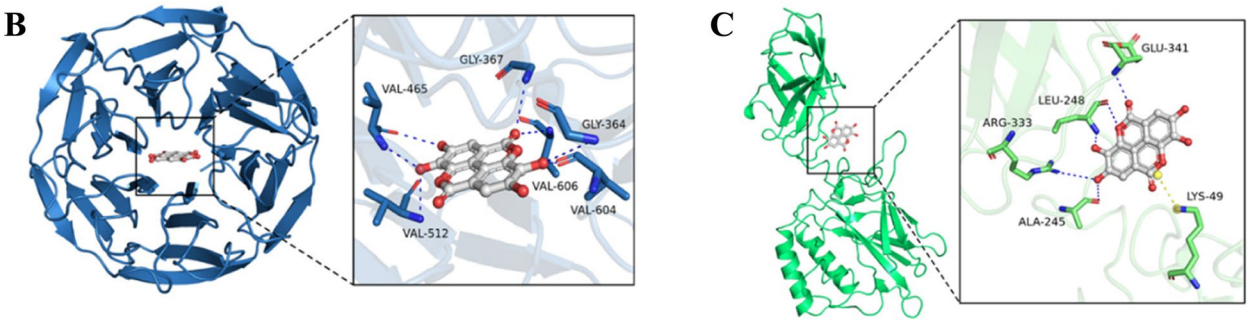

Fig. 6 Binding mode of EA with Keap1, Nrf2, and p65NF-κB determined by molecular docking. **A** The binding energy of EA with potential targets. **B** and **C**, The binding models and corresponding 2D figures showing the interactions of EA with the Keap1 (**B**) and p65NF-κB (**C**) proteins

inflammatory responses both in vitro and in vivo [28, 31–34]. Furthermore, our current data showed that EA supplementation could effectively reverse the CDDP exposure-induced upregulation of lipid peroxidation, caspase activity, and the inflammatory response in the livers of mice, and these protective effects might be partly dependent on the regulation of the NF-κB pathway and Nrf2/HO-1 pathway (Figs. 1, 2, 3, 4 and 5).

Excessive ROS production caused by CDDP exposure can directly damage intracellular macromolecules (e.g., lipids, DNA, and proteins) and subcellular organelles (e.g., mitochondria, the endoplasmic reticulum, and lysosomes), triggering cell death [3, 6, 35, 36]. These findings are a critical molecular basis of CDDP-induced toxicity in animals and humans [35]. It has been demonstrated that inhibition of ROS production and oxidative stress via antioxidant supplementation can partly attenuate CDDP-induced cell apoptosis and ototoxicity [37]. Our current results revealed that CDDP exposure significantly upregulated MDA levels and significantly downregulated SOD and CAT activities in the livers of mice (Fig. 3). The antioxidant enzymes SOD and CAT can directly catalyze superoxide anion, and hydrogen peroxide (H_2O_2) is a nontoxic substance in eukaryotic cells and plays vital roles in the process of antioxidative stress [38]. MDA is one biomarkers of lipid peroxidation [39]. This evidence indicated that CDDP exposure could lead to oxidative damage in the liver tissues of mice via the inhibition of antioxidant enzyme activities. Moreover, our data revealed that EA co-treatment at final doses of 50 and 100 mg/kg/day partly abolished the increase in MDA and the decrease in SOD and CAT activities in the livers of mice exposed to CDDP (Fig. 3). Similarly, Zhang et al. reported that EA co-treatment (at 100 mg/kg/day for five days) significantly reduced the production of MDA and increased the total antioxidant capacity and the level of GSH-PX activity, subsequently protecting against oxidative damage caused by diquat (a toxic pesticide) exposure in the jejunum tissues of mice [24]. In another study, Zhao et al. found that oral EA administration at doses of 50 and 100 mg/kg/day for four weeks significantly increased the activities of CAT, SOD, and GSH-PX, then protected against chronic ethanol exposure-induced liver injury in mice [40]. This evidence the protective effects of EA on CDDP-caused liver toxicity may be partly dependent on its anti-oxidative stress activity. Mitochondria are also the target of ROS, and dysfunctional mitochondria can increase the release of cytochrome C (CytC), which activates caspases-9 and -3 and ultimately leads to cell apoptosis [41]. Consistently, our current data revealed that EA co-treatment markedly decreased the activities of caspase-9 and caspase-3 in the livers of CDDP-treated mice (Fig. S4). In brief, these data indicated that EA supplementation attenuated CDDP exposure-induced liver toxicity by inhibiting caspase activation-mediated cell apoptosis.

It has been reported that CDDP exposure can induce the production of various proinflammatory factors and chemokines, including high mobility group box-1 (HMGB1), TNF-α, IL-6, IL-1β, chemokine ligand 2

(Ccl2), Ccl7, and the C-X-C motif Ccl2 (Cxcl2) [30]. Several studies have also shown that CDDP administration significantly upregulates the expression of NF-κB, a critical transcription factor in the inflammatory response [30, 42]. NF-κB can transcriptionally activate the expression of various proinflammatory genes, such as L-1β, IL-6, and TNF-α [42]. Our data showed that CDDP exposure significantly upregulated the mRNA and protein expression of these genes (i.e., NF-κB, IL-1β, IL-6, and TNF-α). EA cotreatment effectively inhibited the expression of these genes (Fig. S3, and Figs. 4 and 5). Several studies have demonstrated that EA is a potential inhibitor of NF-κB [28, 43]. For example, EA supplementation effectively inhibited LPS-induced NF-κB activation in THP-1 cells, U937 monocytic cells, and liver tissues of mice [28, 43]. Taken together, this evidence indicated that the inhibitory effects of EA on the NF-κB signaling pathway partly contributed to its anti-inflammatory activities.

In response to oxidative stress and inflammatory damage, Nrf2 can function as a "housekeeping" transcription factor [38, 44]. Under normal conditions, the Nrf2 protein is located mainly in the cytoplasm via a bind with Kelch-like ECH-associated protein 1 (Keap1) at the sites of the ETGE and DLG motifs [44]. Under oxidative stress conditions, the interaction between Nrf2 and Keap1 is disrupted, and the Nrf2 protein enters the nucleus, binds to the ARE, and then transcriptionally activates antioxidant genes, such as CAT, GSH-PX, and HO-1, which usually play protective roles [45]. A recent study showed that Nrf2 knockout in mice significantly exacerbated CDDP exposure-induced acute kidney injury, demonstrating that Nrf2 plays a protective role in CDDP-induced nephrotoxicity [46]. EA is considered a potential activator of Nrf2 [22]. Multiple studies have shown that EA cotreatment can promote the expression of Nrf2 and protect against drug or toxin exposure-induced harmful events both in vitro and in vivo [23, 28, 47, 48]. Gu et al. reported that EA pretreatment (at 20 mg/kg, oral administration) significantly activated the expression of Nrf2 and HO-1 proteins and significantly inhibited the expression of NF-κB and TNF-α protein, then markedly ameliorated LPS/D-galactosamine co-exposure-caused acute liver injury in mice [32]. Wei et al. demonstrated that Nrf2 is key target in the protective effects of EA on rotenone-induced neurotoxicity in mice [49]. Our current data revealed that EA cotreatment significantly upregulated the expression of Nrf2 and HO-1 mRNAs and proteins in the livers of mice (Figs. 4 and 5). This evidence indicated that the activation of the Nrf2/HO-1 pathway may play a critical role. Additionally, Nrf2 can partially inhibit the activation of NF-κB via its downstream gene HO-1 [50]. A recent study found that pharmacological inhibition of Nrf2 reduced the protective effect of EA on IL-1β-induced oxidative stress and the inflammatory response in human C28/I2 chondrocytes [23]. These data suggested that the activation of the Nrf2 pathway by EA supplementation may also contribute to its inhibitory effect on the expression of NF-κB. The underlying molecular mechanisms still require further study. In addition, in the present study, molecular docking analysis revealed that the binding energies of EA to the Keap1 and NF-kB proteins were lower than those of the Nrf2 protein, indicating that the stable binding of EA to the Keap1 and NF-kB proteins was greater than that to the Nrf2 protein (Fig. 6).

Importantly, EA has outstanding safety and has been used in food production as a food additive [51, 52]. Tasaki and colleagues reported that the no-observed-effect level (NOEL) of EA in male and female F344 rats was 3011 and 3254 mg/kg body weight/day, respectively [51]. In addition, a previous study reported that oral EA administration at a dosage of 10 mg/kg/day for ten days markedly attenuated CDDP-induced renal dysfunction and oxidative stress damage in rats [53]. Recently, Gao et al. showed that oral EA supplementation at 50 mg/kg/day for seven days improved the CDDP-induced inflammatory response in a mouse model [54]. Taken together, these findings indicated that EA may be a potential protective agent against CDDP-induced toxicity, and further commercial development could be considered.

Conclusions

In a short, our current findings revealed that EA supplementation could effectively ameliorate liver toxicity caused by CDDP exposure, and the underlying molecular mechanisms may involve the inhibition of oxidative stress and the inflammatory response. The potential molecular mechanisms involved the opposite regulation on the NF-κB and Nrf2/HO-1 signaling pathways (Fig. S5). Our current study also shed that EA is a potential anticancer agent for the treatment of CDDP-induced acute liver injury.

Materials and methods

Drugs and reagents

Carboxyl methyl cellulose sodium (CMC-Na) and CDDP (CAS number: 15663–27-1, purity ≥ 99%) were both obtained from Sigma (Shanghai, China). Ellagic acid (CAS number: 476–66-4, purity ≥ 96%; EA) was purchased from Aladdin (Shanghai, China). All other reagents were at least analytically pure.

Animals and treatments

All animal experiments from the present study were performed according to the regulations of the Management of Experimental Animals of China Agricultural

University and approved by the Institutional Animal Care and Use Committee of China Agricultural University (Approval number AW02303202-2–14). C57BL/6 mice (8 weeks old, male, 20–22 g) were obtained from Beijing Weitong Lihua Technology Co., Ltd. (Beijing, China). The mice were allowed to adapt for one week before the treatments. During the experiments, all the mice were fed in a standard room environment with room temperature (at 22 ± 3 °C) and relative humidity (at 50%–60%). A 12 h light–12 h dark cycle was used.

Forty-eight mice were randomly divided into the control, CDDP model, EA100 (i.e., EA at 100 mg/kg/day), and CDDP plus EA25, EA50, or EA100 groups ($n = 8$ in each group), and the detailed treatments are shown as follows:

(1) Control group. Mice were intraperitoneally (i.p.) injected with an equal volume of saline for 2 days and orally administered an equivalent volume of 0.5% CMC-Na for seven days.
(2) CDDP alone group. The dose of CDDP was followed to Lu et al. study [8]. CDDP was dissolved in saline at a final concentration of 2 mg/mL. During the first two days, the mice were i.p. injected with CDDP at a final dose of 20 mg/kg/day (i.e., the cumulative dose was 40 mg/kg). After 2 h, the mice were treated intragastrically with an equal volume of 0.5% CMC-Na (i.e., 0.1 mL/10 g body weight). On the third day, the mice were intragastrically administered 0.5% CMC-Na alone for an additional five days.
(3) EA group. EA was dissolved in 0.5% CMC-Na and prepared as a suspension at a final concentration of 10 mg/mL. Mice were i.p. injected with saline and intragastrically administered EA at a final dosage of 100 mg/kg/day for seven days.
(4)(6) CDDP plus EA 25, EA 50, or EA 100 groups. EA was dissolved in 0.5% CMC-Na and prepared as a suspension at final concentrations of 2.5, 5, and 10 mg/mL. During the first two days, the mice were i.p. injected with CDDP at a final dose of 20 mg/kg per day (i.e., the cumulative dose was 40 mg/kg). After 2 h, the mice were intragastrically administered EA at final doses of 25, 50, or 100 mg/kg per day (0.1 mL/10 g body weight). On the third day, the mice were continually administered EA intragastrically at final doses of 25, 50, or 100 mg/kg per day for an additional five days.

At 12 h after the last dose of EA, the mice were sacrificed with a higher dose of pentobarbital sodium by intraperitoneal injection at a dose of 80 mg/kg body weight. Blood was collected from each mouse for biochemical analysis, and liver tissue was collected for histopathological examination and measurement of protein and gene expression.

Liver index

After the mice were anesthetized and euthanized, the liver tisues were quickly isolated and their weight was recorded. The liver index was calculated. As followes: liver index = (liver weight/body weight) × 100%.

Measurement of serum biochemistry

The blood sample of each mouse was collected, then, they were centrifuged at 3000 × g for 15 min at room temperature. The obtained serum was used to determinate the levels of serum aspartate aminotransferase (AST) and alanine aminotransferase (ALT). An automatic analyzer (Hitachi 7080, Tokyo, Japan) coupled with standard AST and ALT diagnostic kits (Kehua Biological Engineering Company, Shanghai, China) was used, according to our previous study [55].

Histopathological analysis

Four livers from each treatment group were selected for histopathological examination, and the detailed protocols used were described in a previous study [39]. In brief, the isolated liver tissues were fixed in 10% neutral formalin solution. After 48 h, the samples were dehydrated, cleared, paraffin embedded, and sectioned. Then, a hematoxylin–eosin (H&E) staining was carried out. The histological parameters of hepatocyte necrosis and inflammation were scored according to Taghizadeh et al. study [36]. As follows: 0, normal (there was no observed pathological damage); 1, mild (minor damage with a few hepatocyte necroses and inflammatory cell infiltration); 2, moderate (pathological damage degree between scores 1 and 3); or 3, severe (numerous liver cell necrosis and inflammatory cell infiltration). In each slice, 15 images were analyzed, and the average value was calculated.

Measurements of MDA, CAT, and SOD levels

Commercial MDA (catalog number: A003-1–2), CAT (catalog number: A007-1–1), and SOD (catalog number: A001-3–2) kits (Nanjing Jiancheng, Nanjing, China) were used to measure the MDA levels and the CAT and SOD activities in the livers of the mice, respectively, according to the manufacturer's instructions. The protein concentration of each sample was measured by a BCA™ protein assay kit (Beyotime, Haimen, China).

Measurements of inflammatory markers

The levels of TNF-a, IL-1β, and IL-6 in the liver tissues were measured by using commercial TNF-a, IL-1β, and IL-6 ELISA kits (R&D Systems, Minneapolis, MN, United States). The protein concentration of each sample

was measured by a BCA™ protein assay kit (Beyotime, Haimen, China).

Measurements of caspase-9 and caspase-3 activities

The relative activities of caspase-9 and caspase-3 in the liver were determined using commercial caspase-9 and caspase-3 kits (Beyotime, Haimen, China), respectively. The detail protocol was shown in Suppl. Material and Methods.

Quantitative RT–PCR

Total RNA was isolated using a Total RNA Isolation Kit (Vazyme Biotech Co., Ltd., Nanjing, China) according to the manufacturer's instructions. The detailed protocols for cDNA synthesis and quantitative RT–PCR are described in the Suppl. Material and Methods. The primer information is presented in Table S1.

Western blotting

To analyze the expression of the target proteins, Western blotting was carried out according to the protocols described in our previous study [56]. In brief, 20 mg of liver tissue from each sample was crushed and lysed in ice-cold RIPA buffer supplemented with various protein inhibitors (i.e., 0.5 mM Na_3VO_4, 50 mM NaF, and 1 μg/mL PMSF). An automatic low-temperature crusher (Seville Company, Wuhan, China) was used under 30 W working conditions (each cycle: 5 s of ultrasonication and 3 s of pause; 6 cycles per sample). After ultrasonication, the samples were centrifuged using a refrigerated centrifuge (12,000 rpm for 15 min; 4 °C), the supernatants of each sample were isolated, and the corresponding protein concentrations were quantified via a BCA™ protein assay kit. Twenty micrograms of protein from each sample were loaded and separated using a commercial SDS–PAGE Precast Gel (Beyotime, Haimen, China). Primary antibodies, including rabbit antibodies against Nrf2, HO-1 (1:1000 dilution; Proteintech, Chicago, United States), and p65NF-κB (1:1000 dilution; Santa Cruz, CA, United States) and mouse antibodies against β-actin (1:1000 dilution; Santa Cruz, CA, United States), were used. The relative protein expression in each gel was analyzed using Image J software (V1.8.0.112, NIH, MD, USA).

Molecular docking analysis

The binding affinities and modes of interaction between EA and the Nrf2, Keap1, and NF-kB proteins were analyzed using an AutodockVina 1.2.2 software. The 2D coordinates of mouse Nrf2 (UniProt: Q60795), Keap1 (UniProt: Q9Z2X8), and p65NF-kB (UniProt: P25799) proteins were downloaded via the PDB website, and the molecular docking studies were conducted using an AutoDock Vina 1.2.2 software (NIH, MD, USA).

Statistical analysis

All data in the current study were analyzed using GraphPad 9.0 software (Dotmatics Company, Boston, MA, USA). The results are presented as the mean ± standard deviation (S.D.). The statistical analysis between any two groups was carried out using one-way analysis of variance (ANOVA) with Tukey's multiple comparisons post hoc test. A p value less than 0.05 indicated a significant difference.

Supplementary Information

The online version contains supplementary material available at https://doi.org/10.1186/s44280-024-00056-w.

Supplementary Materials: Table S1. The primer sequences of quantitative RT–PCR. Fig. S1. Chemical structure of ellagic acid (EA). Suppl. Fig. S2. The changes of relative liver weight in mice. Fig. S3. The protein levels of IL-1β (A), TNF-α (B), and IL-6 (C) in the livers of the mice. Fig. S4. Caspase-9 (A) and caspase-3 (B) activities in the livers of the mice. Fig. S5. Schematic diagram of the proposed mechanisms by which EA protects against CDDP exposure-induced liver toxicity.

Authors' contributions

Conceptualization, C.D.; methodology, Q.M., X.Z., Y.L., M.L. and Z.H.; software, X.Z. and S.T.; validation, C.D., and S.T.; formal analysis, Y.L. and C.D.; project administration, C.D.; writing—review and editing, C.D.; funding acquisition, C.D.; investigation, X.Z., and Y.L.; writing—original draft preparation, X.Z. and C.D. All authors reviewed, revised, and approved the final manuscript.

Funding

This study was supported by the National Natural Science Foundation of China (Award number 32102724). This study was also supported by the Special Fund Management Office for Basic Research Business Expenses of China Agricultural University (2023TC028) and the Pinduoduo-China Agricultural University Research Fund (Grant No. PC2023A01002).

Availability of data and materials

The data will be shared upon request by the readers.

Declarations

Ethics approval and consent to participate

In the present study, all animal experiments were performed according to the regulations of the Management of Experimental Animals of China Agricultural University and approved by the Institutional Animal Care and Use Committee of China Agricultural University (Approval number AW02303202-2–14).

Competing interests

All the authors declare that there are no conflicts of interest related to this manuscript.

Received: 20 December 2023 Revised: 18 June 2024 Accepted: 1 July 2024
Published online: 29 July 2024

References

1. Shen DW, Pouliot LM, Hall MD, Gottesman MM. Cisplatin resistance: a cellular self-defense mechanism resulting from multiple epigenetic and genetic changes. Pharmacol Rev. 2012;64(3):706–21.

2. Hill NO. Cis-platinum for cancer. N Engl J Med. 1979;301(1):47.
3. Tang C, Livingston MJ, Safirstein R, Dong Z. Cisplatin nephrotoxicity: new insights and therapeutic implications. Nat Rev Nephrol. 2023;19(1):53–72.
4. Squillace S, Niehoff ML, Doyle TM, Green M, Esposito E, Cuzzocrea S, et al. Sphingosine-1-phosphate receptor 1 activation in the central nervous system drives cisplatin-induced cognitive impairment. J Clin Invest. 2022;132(17):e157738.
5. Nofal AE, Okdah YA, Rady MI, Hassaan HZ. Gum acacia attenuates cisplatin toxic effect spermatogenesis dysfunction and infertility in rats. Int J Biol Macromol. 2023;240:124292.
6. Rottenberg S, Disler C, Perego P. The rediscovery of platinum-based cancer therapy. Nat Rev Cancer. 2021;21(1):37–50.
7. Al-Malki AL, Sayed AA. Thymoquinone attenuates cisplatin-induced hepatotoxicity via nuclear factor kappa-β. BMC Complement Altern Med. 2014;14:282.
8. Lu Y, Cederbaum AI. Cisplatin-induced hepatotoxicity is enhanced by elevated expression of cytochrome P450 2E1. Toxicological sciences : an official journal of the Society of Toxicology. 2006;89(2):515–23.
9. Elhady SS, Abdelhameed RFA, Mehanna ET, Wahba AS, Elfaky MA, Koshak AE, et al. Metabolic profiling, chemical composition, antioxidant capacity, and in vivo hepato- and nephroprotective effects of sonchus cornutus in mice exposed to cisplatin. Antioxidants (Basel). 2022;11(5):819.
10. Habib SA, Suddek GM, Abdel Rahim M, Abdelrahman RS. The protective effect of protocatechuic acid on hepatotoxicity induced by cisplatin in mice. Life Sci. 2021;277:119485.
11. Hong KO, Hwang JK, Park KK, Kim SH. Phosphorylation of c-Jun N-terminal Kinases (JNKs) is involved in the preventive effect of xanthorrhizol on cisplatin-induced hepatotoxicity. Arch Toxicol. 2005;79(4):231–6.
12. Omar HA, Mohamed WR, Arab HH, Arafa el SA. Tangeretin alleviates cisplatin-induced acute hepatic injury in rats: targeting MAPKs and apoptosis. PLoS One. 2016;11(3):e0151649.
13. Sami DH, Soliman AS, Khowailed AA, Alruhaimi RS, Hassanein EHM, Kamel EM, et al. The protective effect of 7-hydroxycoumarin against cisplatin-induced liver injury is mediated via attenuation of oxidative stress and inflammation and upregulation of Nrf2/HO-1 pathway. Environ Sci Pollut Res Int. 2023;30(33):80181–91.
14. Lin Q, Li S, Jin H, Cai H, Zhu X, Yang Y, et al. Mitophagy alleviates cisplatin-induced renal tubular epithelial cell ferroptosis through ROS/HO-1/GPX4 axis. Int J Biol Sci. 2023;19(4):1192–210.
15. Cho SI, Lee JE, Do NY. Protective effect of silymarin against cisplatin-induced ototoxicity. Int J Pediatr Otorhinolaryngol. 2014;78(3):474–8.
16. Mansour HH, Hafez HF, Fahmy NM. Silymarin modulates cisplatin-induced oxidative stress and hepatotoxicity in rats. J Biochem Mol Biol. 2006;39(6):656–61.
17. Abdelmeguid NE, Chmaisse HN, Abou Zeinab NS. Silymarin ameliorates cisplatin-induced hepatotoxicity in rats: histopathological and ultrastructural studies. Pak J Biol Sci. 2010;13(10):463–79.
18. Chi MY, Zhang H, Wang YX, Sun XP, Yang QJ, Guo C. Silibinin alleviates muscle atrophy caused by oxidative stress induced by cisplatin through ERK/FoxO and JNK/FoxO pathways. Oxid Med Cell Longev. 2022;2022:5694223.
19. Kim DH, Sim Y, Hwang JH, Kwun IS, Lim JH, Kim J, et al. Ellagic acid prevents binge alcohol-induced leaky gut and liver injury through inhibiting gut dysbiosis and oxidative stress. Antioxidants (Basel). 2021;10(9):1386.
20. Azam F, Khan MA, Khan A, Ahmad S, Zofair SFF, Younus H. In silico and in vitro studies on the inhibition of laccase activity by Ellagic acid: implications in drug designing for the treatment of Cryptococcal infections. Int J Biol Macromol. 2022;209(Pt A):642–54.
21. Yoganathan S, Alagaratnam A, Acharekar N, Kong J. Ellagic acid and schisandrins: natural biaryl polyphenols with therapeutic potential to overcome multidrug resistance in cancer. Cells. 2021;10(2):458.
22. Wang Q, Botchway BOA, Zhang Y, Liu X. Ellagic acid activates the Keap1-Nrf2-ARE signaling pathway in improving Parkinson's disease: A review. Biomed Pharmacother. 2022;156:113848.
23. Zhu W, Tang H, Li J, Guedes RM, Cao L, Guo C. Ellagic acid attenuates interleukin-1β-induced oxidative stress and exerts protective effects on chondrocytes through the Kelch-like ECH-associated protein 1 (Keap1)/Nuclear factor erythroid 2-related factor 2 (Nrf2) pathway. Bioengineered. 2022;13(4):9233–47.
24. Zhang X, Wang S, Wu Y, Liu X, Wang J, Han D. Ellagic acid alleviates diquat-induced jejunum oxidative stress in C57BL/6 mice through activating Nrf2 mediated signaling pathway. Nutrients. 2022;14(5):1103.
25. Aishwarya V, Solaipriya S, Sivaramakrishnan V. Role of ellagic acid for the prevention and treatment of liver diseases. Phytother Res. 2021;35(6):2925–44.
26. Kang EH, Kown TY, Oh GT, Park WF, Park SI, Park SK, et al. The flavonoid ellagic acid from a medicinal herb inhibits host immune tolerance induced by the hepatitis B virus-e antigen. Antiviral Res. 2006;72(2):100–6.
27. Qi M, Wang N, Xiao Y, Deng Y, Zha A, Tan B, et al. Ellagic acid ameliorates paraquat-induced liver injury associated with improved gut microbial profile. Environ Pollut. 2022;293:118572.
28. Aslan A, Gok O, Erman O, Kuloglu T. Ellagic acid impedes carbontetrachloride-induced liver damage in rats through suppression of NF-kB, Bcl-2 and regulating Nrf-2 and caspase pathway. Biomed Pharmacother. 2018;105:662–9.
29. Aslan A, Gok O, Beyaz S, Ağca CA, Erman O, Zerek A. Ellagic acid prevents kidney injury and oxidative damage via regulation of Nrf-2/NF-κB signaling in carbon tetrachloride induced rats. Mol Biol Rep. 2020;47(10):7959–70.
30. Gong S, Feng Y, Zeng Y, Zhang H, Pan M, He F, et al. Gut microbiota accelerates cisplatin-induced acute liver injury associated with robust inflammation and oxidative stress in mice. J Transl Med. 2021;19(1):147.
31. Devipriya N, Sudheer AR, Srinivasan M, Menon VP. Effect of ellagic acid, a plant polyphenol, on fibrotic markers (MMPs and TIMPs) during alcohol-induced hepatotoxicity. Toxicol Mech Methods. 2007;17(6):349–56.
32. Gu L, Deng WS, Liu Y, Jiang CH, Sun LC, Sun XF, et al. Ellagic acid protects Lipopolysaccharide/D-galactosamine-induced acute hepatic injury in mice. Int Immunopharmacol. 2014;22(2):341–5.
33. Beigi T, Safi A, Satvati M, Kalantari-Hesari A, Ahmadi R, Meshkibaf MH. Protective role of ellagic acid and taurine against fluoxetine induced hepatotoxic effects on biochemical and oxidative stress parameters, histopathological changes, and gene expressions of IL-1β, NF-κB, and TNF-α in male Wistar rats. Life Sci. 2022;304:120679.
34. Cuevas-Magaña MY, Vega-García CC, León-Contreras JC, Hernández-Pando R, Zazueta C, García-Niño WR. Ellagic acid ameliorates hexavalent chromium-induced renal toxicity by attenuating oxidative stress, suppressing TNF-α and protecting mitochondria. Toxicol Appl Pharmacol. 2022;454:116242.
35. Gentilin E, Simoni E, Candito M, Cazzador D, Astolfi L. Cisplatin-induced ototoxicity: updates on molecular targets. Trends Mol Med. 2019;25(12):1123–32.
36. Taghizadeh F, Hosseinimehr SJ, Zargari M, Karimpour Malekshah A, Mirzaei M, Talebpour AF. Alleviation of cisplatin-induced hepatotoxicity by gliclazide: Involvement of oxidative stress and caspase-3 activity. Pharmacol Res Perspect. 2021;9(3):e00788.
37. Kim KH, Lee B, Kim YR, Kim MA, Ryu N, Jung DJ, et al. Evaluating protective and therapeutic effects of alpha-lipoic acid on cisplatin-induced ototoxicity. Cell Death Dis. 2018;9(8):827.
38. Zhang X, Liu Y, Shen Z, Wang S, Wu C, Liu D, et al. Osthole ameliorates myonecrosis caused by *Clostridium perfringens* type A infection in mice. One Health Adv. 2023;1(1):27.
39. Dai C, Zhang X, Lin J, Shen J. Nootkatone supplementation ameliorates carbon tetrachloride-induced acute liver injury via the inhibition of oxidative stress, NF-κB pathways, and the activation of Nrf2/HO-1 pathway. Antioxidants (Basel). 2023;12(1):194.
40. Zhao L, Mehmood A, Soliman MM, Iftikhar A, Iftikhar M, Aboelenin SM, et al. Protective effects of ellagic acid against alcoholic liver disease in mice. Front Nutr. 2021;8:744520.
41. Green DR, Reed JC. Mitochondria and apoptosis. Science. 1998;281(5381):1309–12.
42. Fu Y, Xiang Y, Wang Y, Liu Z, Yang D, Zha J, et al. The STAT1/HMGB1/NF-κB pathway in chronic inflammation and kidney injury after cisplatin exposure. Theranostics. 2023;13(9):2757–73.
43. Rønning SB, Voldvik V, Bergum SK, Aaby K, Borge GIA. Ellagic acid and urolithin A modulate the immune response in LPS-stimulated U937 monocytic cells and THP-1 differentiated macrophages. Food Funct. 2020;11(9):7946–59.
44. Bello M, Morales-González JA. Molecular recognition between potential natural inhibitors of the Keap1-Nrf2 complex. Int J Biol Macromol. 2017;105(Pt 1):981–92.

45. Tonelli C, Chio IIC, Tuveson DA. Transcriptional regulation by Nrf2. Antioxid Redox Signal. 2018;29(17):1727–45.
46. Hu J, Gu W, Ma N, Fan X, Ci X. Leonurine alleviates ferroptosis in cisplatin-induced acute kidney injury by activating the Nrf2 signalling pathway. Br J Pharmacol. 2022;179(15):3991–4009.
47. Xiao Y, Huang R, Wang N, Deng Y, Tan B, Yin Y, et al. Ellagic acid alleviates oxidative stress by mediating Nrf2 Signaling pathways and protects against paraquat-induced intestinal injury in piglets. Antioxidants (Basel). 2022;11(2):252.
48. Ding X, Jian T, Wu Y, Zuo Y, Li J, Lv H, et al. Ellagic acid ameliorates oxidative stress and insulin resistance in high glucose-treated HepG2 cells via miR-223/keap1-Nrf2 pathway. Biomed Pharmacother. 2019;110:85–94.
49. Wei YZ, Zhu GF, Zheng CQ, Li JJ, Sheng S, Li DD, et al. Ellagic acid protects dopamine neurons from rotenone-induced neurotoxicity via activation of Nrf2 signalling. J Cell Mol Med. 2020;24(16):9446–56.
50. Gao W, Guo L, Yang Y, Wang Y, Xia S, Gong H, et al. Dissecting the crosstalk between Nrf2 and NF-κB response pathways in drug-induced toxicity. Frontiers in cell and developmental biology. 2021;9:809952.
51. Tasaki M, Umemura T, Maeda M, Ishii Y, Okamura T, Inoue T, et al. Safety assessment of ellagic acid, a food additive, in a subchronic toxicity study using F344 rats. Food Chem Toxicol. 2008;46(3):1119–24.
52. Heilman J, Andreux P, Tran N, Rinsch C, Blanco-Bose W. Safety assessment of Urolithin A, a metabolite produced by the human gut microbiota upon dietary intake of plant derived ellagitannins and ellagic acid. Food Chem Toxicol. 2017;108(Pt A):289–97.
53. Ateşşahín A, Ceríbaşi AO, Yuce A, Bulmus O, Cikim G. Role of ellagic acid against cisplatin-induced nephrotoxicity and oxidative stress in rats. Basic Clin Pharmacol Toxicol. 2007;100(2):121–6.
54. Gao Y, Peng K, Wang Y, Guo Y, Zeng C, Hua R, et al. Ellagic acid ameliorates cisplatin-induced acute kidney injury by regulating inflammation and SIRT6/TNF-α signaling. Food Sci Human Wellness. 2023;12(6):2232–41.
55. Dai C, Liu M, Zhang Q, Das Gupta S, Tang S, Shen J. Nootkatone Supplementation attenuates carbon tetrachloride exposure-induced nephrotoxicity in mice. Antioxidants (Basel). 2023;12(2):370.
56. Dai C, Zhang Q, Shen L, Sharma G, Jiang H, Wang Z, et al. Quercetin attenuates quinocetone-induced cell apoptosis in vitro by activating the P38/Nrf2/HO-1 pathway and inhibiting the ROS/Mitochondrial apoptotic pathway. Antioxidants (Basel). 2022;11(8):1498.

Publisher's Note